Characterizing intra-exciton Coulomb scattering in terahertz excitations

S. Zybell, J. Bhattacharyya, S. Winnerl, F. Eßer, M. Helm, H. Schneider, L. Schneebeli, C. N. Böttge, M. Kira, S. W. Koch, A. M. Andrews, and G. Strasser

Articles you may be interested in

Light emission lifetimes in p-type δ-doped GaAs/AlAs multiple quantum wells near the Mott transition
J. Appl. Phys. **112**, 043105 (2012); 10.1063/1.4745893

Efficiency of light emission in high aluminum content AlGaN quantum wells
J. Appl. Phys. **105**, 073103 (2009); 10.1063/1.3103321

Photoluminescence modulation by high-frequency lateral electric fields in quantum wells
Appl. Phys. Lett. **78**, 1559 (2001); 10.1063/1.1355292

Excitonic photoluminescence in a shallow quantum well under electric field
Appl. Phys. Lett. **72**, 1217 (1998); 10.1063/1.121018

Characterization of photoluminescence intensity and efficiency of free excitons in semiconductor quantum well structures
J. Appl. Phys. **82**, 3870 (1997); 10.1063/1.365689

Characterizing intra-exciton Coulomb scattering in terahertz excitations

S. Zybell,[1,2] J. Bhattacharyya,[1] S. Winnerl,[1] F. Eßer,[1,2] M. Helm,[1,2] H. Schneider,[1,a)]
L. Schneebeli,[3] C. N. Böttge,[3] M. Kira,[3] S. W. Koch,[3] A. M. Andrews,[4] and G. Strasser[4]

[1]Helmholtz-Zentrum Dresden-Rossendorf, P.O. Box 510119, 01314 Dresden, Germany
[2]Technische Universität Dresden, 01062 Dresden, Germany
[3]Department of Physics and Material Sciences Center, Philipps-Universität Marburg,
Renthof 5, 35032 Marburg, Germany
[4]Institute for Solid State Electronics and Center for Micro- and Nanostructures, Vienna University of
Technology, Floragasse 7, 1040 Vienna, Austria

An intense terahertz field is applied to excite semiconductor quantum wells yielding strong non-equilibrium exciton distributions. Even though the relaxation channels involve a complicated quantum kinetics of Coulomb and phonon effects, distinct relaxation signatures of Coulomb scattering are identified within time-resolved photoluminescence by comparing the experiment with a reduced model that contains all relevant microscopic processes. The analysis uncovers a unique time scale for the Coulomb scattering directly from experiments and reveals the influence of phonon relaxation as well as radiative decay. © 2014 AIP Publishing LLC. [http://dx.doi.org/10.1063/1.4902431]

High-quality semiconductor quantum wells (QWs), especially in GaAs/AlGaAs material systems, provide the opportunity to study the internal structure of excitons.[1–4] These Coulomb-bound electron–hole pairs form hydrogen-atom–like states with transition energies matching the terahertz (THz) frequencies (1 THz corresponds to 4.1 meV). In particular, the $1s - 2p$ transition (in hydrogen notation) represents an effective two-level system which can be excited by strong THz fields, leading to phenomena like ac Stark effect,[2] high-order-sideband generation,[3] and excitonic ionization.[4] As shown both theoretically[5] and experimentally,[6] Coulomb scattering between the nearly energetically degenerate $2s$ and $2p$ states is extremely efficient. While $2p$ excitons cannot recombine radiatively, a $1s$-to-$2p$ excitation also generates $2s$ excitons through such a Coulomb scattering, which was experimentally detected as excess $2s$ photoluminescence.[6]

In the present work, we investigate the decay of the excess $2s$ photoluminescence (PL) as well as thermalization of the system after a strong THz pulse has excited the $1s$-to-$2p$ transition. We show that the THz excitation strongly disturbs the initial dominant $1s$-exciton population by quenching the $1s$ population and generating $2p$, $2s$, and ionized populations, thus creating a non-equilibrium exciton distribution. The resulting interplay between Coulomb- and phonon scattering leads to nontrivial exciton dynamics. We compare the measured results with a theoretical model that includes all relevant microscopic processes and show that one can isolate the Coulomb-relaxation channel through time-resolved PL measurements. In particular, the unique Coulomb-relaxation channel is identified from temporal features of the $1s$- and $2s$-PL intensity. We also discuss qualitatively the influence of phonon relaxation and radiative decay.

Our sample contains 60 QWs with 8.2-nm wide GaAs wells separated by 19.6-nm wide $Al_{0.34}Ga_{0.66}As$ barriers. The $1s$ heavy-hole exciton has an absorption linewidth of

less than 3 meV.[1] The sample is mounted in an optical cryostat and cooled to 6 K. We excite the system with a weak nonresonant optical pulse that mainly creates electron-hole plasma.[7] The interactions can form excitons from plasma via a two-step process.[8,9] First, the Coulomb interaction creates a correlated electron–hole plasma where electrons and holes attract each other slightly without forming bound excitons. This process proceeds fast on a picosecond time scale. Second, the coupling to phonons provides a possible channel for converting correlated electron-hole plasma into bound excitons in 100 s of picoseconds.[10,11] With the near-infrared laser tuned to 1.615 eV, electron–hole pairs in the QW are thus non-resonantly excited at relatively low excitation density of about $10^{10} cm^{-2}$ per QW. We delay the THz excitation by about 600 ps, which guarantees the formation of substantial $1s$-exciton population, as shown in Refs. 8 and 12–14. The spectrally narrow THz pulses are provided by a free-electron laser which allows for time resolution of less than 30 ps. The quasi-cw operation mode enables synchronization to table top Ti:Sapphire laser and, thus, for unique two-color experiments with tunable time delay.[15]

The PL is detected with a grating spectrometer connected to a streak camera (Hamamatsu) and CCD. Each of these time- and energy-resolved streak images is compared with a second one taken under identical conditions but with THz excitation. In Fig. 1(a), a streak image is shown with THz excitation. For detailed evaluation discussed below, horizontal profiles are taken along the dashed lines which mark the $2s$ (1.573 eV) and $1s$ (1.564 eV) energies. Figure 1(a) shows that at the arrival time of the THz pulse, defined as time zero, the $1s$ PL is quenched as the $1s$ population is transferred by the absorbed THz photons into higher-energy states, in agreement with earlier experiments.[16–18] Additionally, the THz pulse generates excess $2s$ PL, identifying a genuine many-body signature. As explained in Ref. 6, the Coulomb scattering among excitons mixes the nearly degenerate $2p$ and $2s$ exciton states, which eventually yields a direct $1s$-to-$2s$ transfer, a process that is dipole-forbidden in a non-interacting system. The detected pronounced $2s$ peak is about two orders of magnitude

a)Author to whom correspondence should be addressed. Electronic mail: h.schneider@hzdr.de
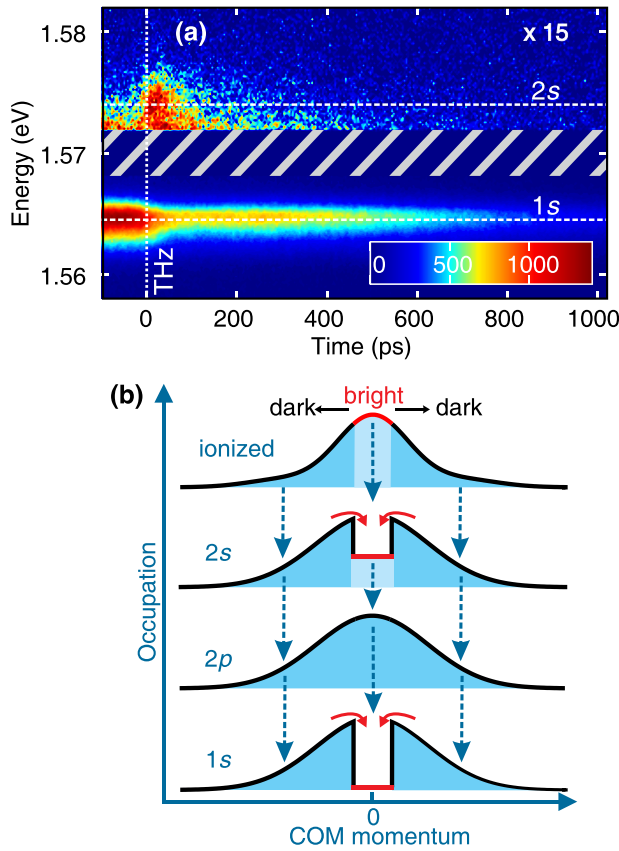
FIG. 1. (a) Streak image of the time-resolved PL with THz excitation at a photon energy of 8.7 meV and 28 nJ/cm^2 THz fluence. The colors indicate the PL intensity and the patterned area marks the filter edge. (b) The center-of-mass distribution is shown for ionized states (top), as well as 2s, 2p, and 1s states (below). The vertical arrows indicate the phonon relaxation while the bent arrows highlight the momentum relaxation between dark and bright exciton states.

weaker than the 1s peak due to the smaller oscillator strength of the excitonic transition.[19] Since our streak camera has a limited dynamic range, direct imaging of both the strong 1s- and the 2s-PL signals simultaneously is not possible. Therefore, a neutral-density filter was installed behind the spectrometer in such a way that only the lower-energy signal (1s) is attenuated, as indicated by the shaded area in Fig. 1(a). Figure 1(a) also shows that the 1s-PL intensity recovers on a long-time scale due to relaxation of excited excitons.

To identify the different processes that contribute to the 1s-PL recovery and the decay of the 2s state, we reduce a microscopic model[5,6] that includes Coulomb scattering, radiative decay, momentum relaxation, and phonon relaxation among exciton states to a rate-equation model for bright and dark exciton densities. The main objective is to reduce the computational effort and to identify physically relevant process rates that can be deduced from the experiment. As a starting point, we "only" compute the initial mix of 1s, 2p, 2s, and other exciton states using the microscopic model of Ref. 6 to determine the exact excitation configuration after a strong THz excitation.

To reveal distinct relaxation channels which influence the exciton's characteristics, the supplementary material (SM)[20] presents the equations of motion that model quantitatively the exciton-density dynamics; also the reduced model is derived based on the full quantum kinetics of excitons presented in

Ref. 7. As a major relaxation mechanism, the radiative exciton-recombination process is highly selective because photon's momentum must match with exciton's center-of-mass (COM) momentum. In GaAs-type systems, the photon momentum q_{ph} is extremely small compared to a typical exciton momentum **q**. Therefore, only a small fraction of excitons can recombine radiatively. Momentum distributions of different excitons during the relaxation process are illustrated schematically in Fig. 1(b); bright (dark) excitons, indicated by red (black) line, have a small (large) momentum inside (beyond) the so-called optical cone $|\mathbf{q}| < q_{ph}$ ($|\mathbf{q}| > q_{ph}$), denoted by bright (dark) shading, such that they can (cannot) recombine radiatively to produce PL. Due to this momentum-selective recombination, the bright excitons decay radiatively (shown by the decreased occupation around $q = 0$ in Fig. 1(b)), while the dark excitons remain in the system for a very long time. However, the scattering from dark to bright excitons not only feeds bright excitons but eventually drains also the dark excitons. Therefore, especially, the 1s-exciton distribution exhibits a strong hole burning at small momenta, as shown in Refs. 7, 21, and 22. Figure 1(b) illustrates schematically the effect of radiative hole burning on different exciton levels. In GaAs-type semiconductors, the radiative decay is fast for the bright 1s excitons, while it is moderate for the 2s excitons and nonexistent for the p-like as well as for dark excitons as indicated by the respective extents of hole burning in Fig. 1(b). Due to superradiant coupling among 60 QWs,[23,24] the radiative decay of bright 1s (2s) excitons is 3 ps (39 ps) that is roughly eight times faster than for a single QW.[23]

As the hole burning proceeds, momentum relaxation among excitons [red horizontal arrows, Fig. 1(b)] replenishes the hole, mainly due to acoustic phonons which represent an additional relaxation channel. We find that our experiments are explained when the momentum-relaxation time is $\tau_{MOM} = 32$ ps. This time is much slower than the hole burning such that the hole remains significant while the overall radiative decay of excitons is slow. The analytical formula for the overall radiative decay, given by

$$\tau_{rad} = (\tau_{rad,1s} + \tau_{MOM})(1 + F), \qquad (1)$$

shows that the used $\tau_{rad,\lambda}$ and τ_{MOM} effects combined yield an overall radiative decay time of 600 ps for all excitons. As outlined in the SM,[20] the factor F defines the ratio of dark versus bright exciton densities and is given by $F = 16$ in our case. Equation (1) shows that the overall PL decay determines only the product of individual relaxation times and F, not the individual $\tau_{rad,1s}$, τ_{MOM}, or F.

The THz excitation itself strongly inverts the system such that phonons are needed to thermalize the system toward the 1s state [dashed arrows, Fig. 1(b)], yielding an independent relaxation channel with time scale τ_{TD}. Our experiments are explained by $\tau_{TD} = 600$ ps thermalization time as shown below. Besides the phonon effects, we also model the Coulomb scattering among 1s, 2s, and 2p excitons based on the theory of Ref. 6. The effective 2s-to-2p conversion time $\tau_c = 100$ ps explains the experiments as shown below. We note that the Coulomb scattering represents another important relaxation mechanism among excitons and is responsible for efficient 1s-to-2s population transfer even

when the THz field is resonant only with the 1s-to-2p transition.

Figure 2 shows an experiment–theory comparison of the 2s-decay and 1s-recovery dynamics. The experimental time traces are obtained through an integration over a ± 2 meV spectral range in Fig. 1(a) along horizontal profiles marked by the dashed lines. We compare measured PL intensities with theoretically computed exciton populations which are proportional to the resulting PL intensity. As discussed above, many processes are simultaneously involved with the quantum kinetics of exciton dynamics, which makes the relaxation a complicated mix of interaction effects. In the following, however, we describe how one can focus on a particular relaxation aspect by following specific measured 1s and 2s PL features to extract the relaxation time τ_c of the Coulomb relaxation. In other words, there is a particular marker within the measured PL that uniquely defines the time constant τ_c.

We focus on the initial fast decay of the 2s-PL dynamics [Fig. 2(b), red] and find that it matches the Coulomb-conversion time τ_c, as indicated by the black dashed line [$\exp(-t/\tau_c)$] in Fig. 2(b). This time scale is determined by the fast Coulomb conversion that mixes the 2s, 2p, and 1s states and relaxes 2s densities into the ground state. Hence, we find that the Coulomb-conversion time τ_c can be extracted by the initial 2s-PL dynamics shortly after the THz-pulse center. Now turning to the recovery of the 1s-PL signal [Fig. 2(d)], this process takes comparatively long, as the temporal maximum between recovery and eventual decay of the 1s-PL is just reached about 0.5 ns after the THz pulse, and is observed to occur with a time constant of 350 ps, as shown in more detail in the SM.[20] According to our theory, this slow-down of the 1s-PL recovery, which has not

been addressed in Ref. 6, is caused by the phonon-relaxation time τ_{TD} which increases the transient occupation of dark states during thermalization. We also find that the tail of the 2s PL [Fig. 2(b), red] and 1s PL [Fig. 2(d), shaded] both decay as $\exp(-t/\tau_{rad})$, such that the overall radiative decay is the dominant process within this dynamical range.

After the different time constants are fixed based on different temporal regions in ΔPL_{1s} and ΔPL_{2s}, we indeed find an excellent agreement with experiment and theory, which shows that the parametrization of complicated relaxation physics works remarkably well. For example, we correctly obtain the decay of the 1s PL without THz field, as well as quenching and shelving which both can be seen in the 1s PL when the THz field is applied. In particular, the ratio of THz-on and THz-off 1s-PL beyond 400 ps [Fig. 2(d), red vs. shaded] yields nearly identical shelving of 1s excitons in experiment and theory. The shelving mechanism is known from other experiments: Due to transient occupation of 2p excitons and other optically dark exciton states, the overall radiative decay is suppressed, which yields excess 1s PL after excitons return toward the ground state.[6,18] Additionally, we observe that the 2s signal shows a two-time decay behavior, as observed previously,[6] with an initial fast decay time of 50 ps due to Coulomb scattering and a subsequent slow decay due to the overall radiative decay and phonon relaxation.

To determine whether Coulomb- and phonon interaction yield nonlinear relaxation when the system is excited far from equilibrium, Fig. 3(a) presents the measured 2s PL for increasing THz fluence for a fixed THz energy of 8.7 meV. Figure 3(a) reveals that there are no significant changes of the 2s-decay times for stronger THz excitation. We have supported this observation via the rate-equation-model which
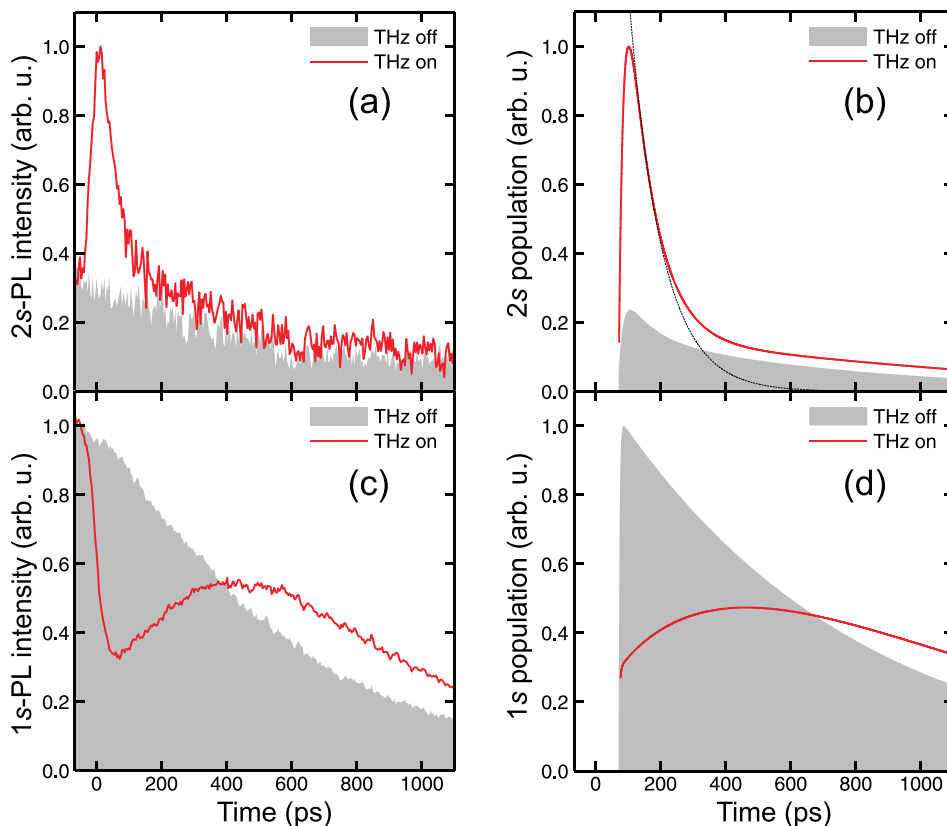

FIG. 2. Measured transient 2s PL (a) and 1s PL (c) for 8.7 meV THz-photon energy excited with 28 nJ/cm^2 THz fluence (solid line) and reference trace (shaded). (b) and (d) are computed population dynamics of 2s and 1s states, respectively. The black line in (b) indicates exponential decay with $\tau_c = 100$ ps.
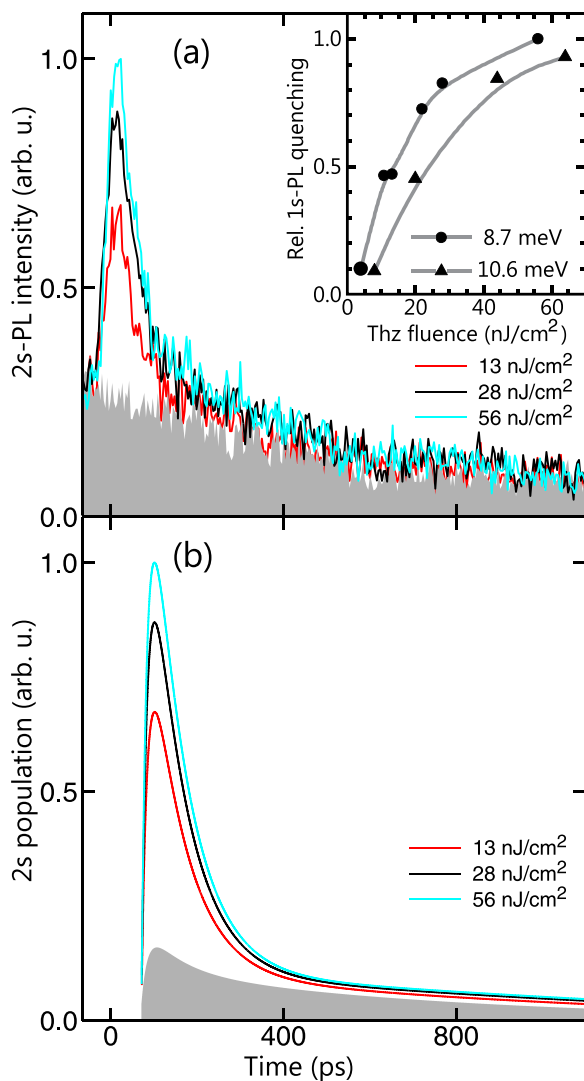
FIG. 3. (a) Measured 2*s* PL for increasing THz fluence (red, black, light blue lines: 13, 28, 56 nJ/cm² from low to high 2*s* PL) and fixed THz energy of 8.7 meV. The shaded area is the THz-off curve. (b) Corresponding computed 2*s* population using same relaxation times for all curves. Inset: relative quenching of 1*s*-PL intensity, as a function of THz fluence Φ_{THz} for two different THz-photon energies 8.7 meV (resonant to 1*s*–2*p* transition, dots) and 10.6 meV (triangles). The gray lines are guides to the eye.

we apply for increasing THz fluence using the *same* relaxation times for all curves, see Fig. 3(b) which shows the computed 2*s* population. We have also checked that the corresponding experiment vs. theory 1*s*-PL curves match very well throughout the excitation range studied when using same relaxation parameters, demonstrating that also the 1*s*-recovery time is independent of the THz-excitation strength.

We next investigate how the relative quenching level Q of the 1*s*-PL signal changes as a function of THz fluence Φ_{THz}; see Fig. 3, inset. For resonant 1*s*–2*p* excitation (8.7 meV), the quenching changes linearly with Φ_{THz} between 0 and 20 nJ/cm² and converges to $Q = 1$, which means 100% depletion of the 1*s* level. For THz-photon energy of 10.6 meV (slightly above resonance), the relative 1*s* quenching shows similar behavior. Note that we study here a large range of THz fluences which leads to large changes in quenching levels. In particular, the blue curve in Figs. 3(a) and 3(b) corresponds to almost a complete quench of 1*s* densities, demonstrating that we can fit the experimental

results throughout a wide excitation regime with the same relaxation parameters.

In conclusion, we have investigated the interplay of Coulomb- and phonon relaxation of THz-induced non-equilibrium exciton distributions. In particular, we have studied the decay of the 2*s* PL and the recovery of the 1*s* PL after resonant THz excitation of 1*s* excitons in GaAs QWs into the 2*p* state and ionization continuum. As the most prominent signature, a fast 2*s*-PL decay with a time constant of 50 ps due to efficient 2*s*–2*p* Coulomb scattering was observed, whereas the recovery of the 1*s* PL was found to take significantly longer because of slow thermalization. We find that the long-time dynamics is dominated by the overall radiative decay. Additionally, the phonon relaxation influences the time when both 1*s*-PL curves (THz on and off) are crossing. We have provided a simple and practical model to extract relaxation rates from experimental data. The reduced model accurately reproduces the main features of the relaxation dynamics and dissolves the complicated quantum kinetics involved among excitons.

[1]M. Wagner, H. Schneider, S. Winnerl, M. Helm, T. Roch, A. M. Andrews, S. Schartner, and G. Strasser, "Resonant enhancement of second order sideband generation for intraexcitonic transitions in GaAs/AlGaAs multiple quantum wells," Appl. Phys. Lett. **94**(24), 241105 (2009).

[2]M. Wagner, H. Schneider, D. Stehr, S. Winnerl, Aaron M. Andrews, S. Schartner, G. Strasser, and M. Helm, "Observation of the intraexciton Autler-Townes Effect in GaAs/AlGaAs semiconductor quantum wells," Phys. Rev. Lett. **105**, 167401 (2010).

[3]B. Zaks, R. B. Liu, and M. S. Sherwin, "Experimental observation of electron–hole recollisions," Nature **483**(7391), 580–583 (2012).

[4]B. Ewers, N. S. Köster, R. Woscholski, M. Koch, S. Chatterjee, G. Khitrova, H. M. Gibbs, A. C. Klettke, M. Kira, and S. W. Koch, "Ionization of coherent excitons by strong terahertz fields," Phys. Rev. B **85**, 075307 (2012).

[5]M. Kira and S. W. Koch, "Exciton-population inversion and terahertz gain in semiconductors excited to resonance," Phys. Rev. Lett. **93**, 076402 (2004).

[6]W. D. Rice, J. Kono, S. Zybell, S. Winnerl, J. Bhattacharyya, H. Schneider, M. Helm, B. Ewers, A. Chernikov, M. Koch, S. Chatterjee, G. Khitrova, H. M. Gibbs, L. Schneebeli, B. Breddermann, M. Kira, and S. W. Koch, "Observation of forbidden exciton transitions mediated by Coulomb interactions in photoexcited semiconductor quantum wells," Phys. Rev. Lett. **110**, 137404 (2013).

[7]M. Kira and S. W. Koch, "Many-body correlations and excitonic effects in semiconductor spectroscopy," Prog. Quantum Electron. **30**, 155–296 (2006).

[8]M. Kira, W. Hoyer, T. Stroucken, and S. W. Koch, "Exciton formation in semiconductors and the influence of a photonic environment," Phys. Rev. Lett. **87**, 176401 (2001).

[9]W. Hoyer, M. Kira, and S. W. Koch, "Influence of Coulomb and phonon interaction on the exciton formation dynamics in semiconductor heterostructures," Phys. Rev. B **67**(15), 155113 (2003).

[10]R. A. Kaindl, M. A. Carnahan, D. Hägele, R. Lövenich, and D. S. Chemla, "Ultrafast terahertz probes of transient conducting and insulating phases in an electron-hole gas," Nature **423**, 734–738 (2003).

[11]M. Kira, W. Hoyer, and S. W. Koch, "Terahertz signatures of the exciton formation dynamics in non-resonantly excited semiconductors," Solid State Commun. **129**(11), 733–736 (2004).

[12]W. Hoyer, C. Ell, M. Kira, S. W. Koch, S. Chatterjee, S. Mosor, G. Khitrova, H. M. Gibbs, and H. Stolz, "Many-body dynamics and exciton formation studied by time-resolved photoluminescence," Phys. Rev. B **72**, 075324 (2005).

[13]R. A. Kaindl, D. Hägele, M. A. Carnahan, and D. S. Chemla, "Transient terahertz spectroscopy of excitons and unbound carriers in quasi-two-dimensional electron–hole gases," Phys. Rev. B **79**, 045320 (2009).

[14]T. Suzuki and R. Shimano, "Exciton Mott transition in Si revealed by terahertz spectroscopy," Phys. Rev. Lett. **109**, 046402 (2012).

[15]J. Bhattacharyya, M. Wagner, S. Zybell, S. Winnerl, D. Stehr, M. Helm, and H. Schneider, "Simultaneous time and wavelength resolved spectroscopy under two-colour near infrared and terahertz excitation," Rev. Sci. Instrum. **82**(10), 103107 (2011).

[16]J. Černe, J. Kono, M. S. Sherwin, M. Sundaram, A. C. Gossard, and G. E. W. Bauer, "Terahertz dynamics of excitons in GaAs/AlGaAs quantum wells," Phys. Rev. Lett. **77**, 1131–1134 (1996).

[17]M. S. Salib, H. A. Nickel, G. S. Herold, A. Petrou, B. D. McCombe, R. Chen, K. K. Bajaj, and W. Schaff, "Observation of internal transitions of confined excitons in GaAs/AlGaAs quantum wells," Phys. Rev. Lett. **77**, 1135 (1996).

[18]S. Zybell, H. Schneider, S. Winnerl, M. Wagner, K. Köhler, and M. Helm, "Photoluminescence dynamics in GaAs/AlGaAs quantum wells

under pulsed intersubband excitation," Appl. Phys. Lett. **99**(4), 041103 (2011).

[19]C. Tanguy, "Optical dispersion by Wannier excitons," Phys. Rev. Lett. **75**, 4090–4093 (1995).

[20]See supplementary material at http://dx.doi.org/10.1063/1.4902431 for the equations of motion that model quantitatively the exciton-density dynamics, and for the numerical fitting of measured data.

[21]S. Chatterjee, C. Ell, S. Mosor, G. Khitrova, H. M. Gibbs, W. Hoyer, M. Kira, S. W. Koch, J. P. Prineas, and H. Stolz, "Excitonic photoluminescence in semiconductor quantum wells: Plasma versus excitons," Phys. Rev. Lett. **92**, 067402 (2004).

[22]M. Kira and S. W. Koch, *Semiconductor Quantum Optics*, 1st ed. (Cambridge University Press, 2011).

[23]M. Kira, F. Jahnke, W. Hoyer, and S. W. Koch, "Quantum theory of spontaneous emission and coherent effects in semiconductor microstructures," Prog. Quantum Electron. **23**(6), 189–279 (1999).

[24]M. Schäfer, W. Hoyer, M. Kira, S. W. Koch, and J. V. Moloney, "Influence of dielectric environment on quantum-well luminescence spectra," J. Opt. Soc. Am. B **25**, 187 (2008).